Electronic Supplementary Material (ESI) for Inorganic Chemistry Frontiers.

Electronic Supplementary Information for:

Asymmetry-Enhanced ^{59}Co NMR Thermometry in Co(III) Complexes

Ökten Üngör, Stephanie Sanchez, Tyler M. Ozvat and Joseph M. Zadrozny

Department of Chemistry, Colorado State University, Fort Collins, Colorado 80523

Inorg. Chem. Front.

Table of Contents

Experimental Section

General Considerations. Complexes **1** and **2** were synthesized with slight modifications to the previous report.[1] Compounds **3** and **4** were purchased from Sigma Aldrich and used after verifying their purity. The asymmetric ligands 2-acetylcycloheptanone (accp) and benzoylacetonate (bzac) were purchased from TCI Chemicals and Oakwood Chemicals, respectively. Cobalt carbonate ($CoCO_3$) was purchased from Alfa Aesar. All reactions are carried out under air.

$Co(accp)_3$ (1) The previously published procedure for $Co(acac)_3$ served as inspiration for the synthesis of this complex.[1] Cobalt carbonate (35.7 mg, 0.3 mmol) and accp (113.5 mg, 0.9 mmol) were heated together for 1 h to 90 °C, resulting in a dark pink slurry solid. 0.75 mL of 10% (w/w) H_2O_2 solution is added drop by drop to the mixture which then became green in color. The mixture is stirred for 15 more minutes until all the effervescence stopped, which indicated a complete reaction. 10 mL of DI water is added to the mixture and the reaction flask is chilled in an ice bath for 5 minutes. The product is collected by vacuum filtration and washed with cold ethanol. A microcrystalline, green powder was obtained (120 mg, 91.4% yield) after drying under a vacuum for 30 min. Dark green, block crystals are grown via slow evaporation from acetonitrile (MeCN) in three days. ^{1}H NMR (δ, 400 MHz, $CDCl_3$): 1.25 (s, 9H), 1.55 (d, 6H), 1.86 (t, 6H), 2.16 (d, 3H), 2.69 (t, 3H), 6.94 (t, 3H). Anal. Calcd. (Found) for $C_{21}H_{30}CoO_6$: 57.67 (57.48) %C and 6.91 (6.24) %H. UV-VIS (CH_2CL_2, 1mM, Fig.2) λmax (nm) (εM (M^{-1} cm^{-1})): 260(33) and 602(60). IR (cm^{-1}, diamond ATR): 447 (Co-O, m), 607 (C-CH_3, m), 732 (C-H, m), 941 (C-C, m), 1162 (C-C, w), 1286 (C-C, s), 1384 (C-H, s), 1470 (C-H, s), 1584 (C=O, vs), 2827, 2965 (C-H, w).

$Co(bzac)_3$ (2) The compound was prepared in the same manner as for **1** from cobalt carbonate (113.5 mg, 0.3 mmol) and bzac (146 mg, 0.9 mmol). Dark green, plate-like crystals were formed after two days from slow evaporation in MeCN (142 mg, 86.7% yield). ^{1}H NMR (δ, 400 MHz, $CDCl_3$): 1.25 (t, 6H), 2.35 (d, 3H), 2.39 (d, 3H), 7.33(q, 9H), 7.41 (t, 3H), 7.86 (q, 6H). Anal. Calcd. (Found) for $C_{30}H_{30}CoO_6$: 66.06 (66.04) %C and 5.54 (5.19) %H. UV-VIS (CH_2Cl_2, 1mM, Fig.S1) λmax (nm) (εM (M^{-1} cm^{-1})): 285(11) and 594(52). IR (cm^{-1}, diamond ATR): 460 (Co-O,

s), 637,674 (C-CH_3, m), 767 (C-H, m), 932 (C-C, m), 1017 (C-C, w), 1356, 1376 (C-C, s), 1516 (C=O, vs), 2342, 2364 (C-H, w), 2827, 2965 (C-H, w).

X-ray Data Collection, Structure Solution, and Refinement for 1. Single-crystal X-ray diffraction data were collected at the X-Ray Diffraction facility of the Analytical Resources Core at Colorado State University. Data for **1** was collected at 300 K on a Bruker D8 Quest ECO single-crystal X-ray diffractometer equipped with Mo Kα (λ = 0.71073 Å). Data were collected and integrated using Bruker Apex 3 software. Absorption corrections were applied using SADABS.[2] Space group assignments were determined by examination of systematic absences, E7 statistics, and successive refinement of the structures. Crystal structures were solved using SHELXT and refined with the aid of successive difference Fourier maps by SHELXL operated in conjunction with OLEX2 software.[3-5] Hydrogen atoms were placed in ideal positions and refined using a riding model for all structures. The crystallographic information file for 1 is available in the CSD at accession number 2238047.

Variable Temperature ^{59}Co NMR Measurements. Samples of **1-4** were made as 0.7 mL volumes of 1-, 10- and 100-mM concentrations in CH_2Cl_2, $CHCl_3$, MeOH, DMSO and 1,2,4-trichlorobenzene (TCB) solvents. Deuteration-dependence of the ^{59}Co NMR peak was studied in $CDCl_3$ and CD_2Cl_2. Spectroscopic measurements were made at 118 MHz (^{59}Co) using an Agilent Unity INOVA 500 MHz (^{1}H) spectrometer at a field strength of 11.74 T with a 5 mm broadband NMR probe. Prior to measurement, the spectrometer was locked to the ^{2}H signal of a 1 M $K_3[Co(CN)_6]$ in D_2O standard to ensure that differences in resonances were not continually affected by a drifting magnetic field. Individual ^{59}Co chemical shifts are all referenced to $K_3[Co(CN)_6]$. Prior to ^{59}Co-NMR experiments, shimming and locking were not performed on the instrument due to the instrument's long-term field stability. In traditional NMR experiments, the resonance peaks are broader due to the absence of shimming and locking. However, due to the rapid collection times of our ^{59}Co experiments, the impact of the broadening on the linewidth of 1-4 is negligible. Each sample was measured across a temperature range of 5-30 °C in a 2°C interval. For each regulated temperature interval, samples were allowed to thermally equilibrate for 5 min before any subsequent measurement. Inversion recovery experiments were made on each sample at 25 °C. Inversion recovery data were acquired from 180° − τ − 90° pulse sequence experiments with 180° and 90° pulse lengths set at 22.4 and 11.2 μs, respectively. Similarly,

CPMG (Carr–Purcell–Meiboom–Gill) pulse sequence experiments were made on each sample at 25 °C. CPMG data were acquired from $90° - (\tau - 180° - \tau)_n$ spin echo pulse sequence experiments with 180° and 90° pulse lengths identical to the corresponding inversion recovery parameters.

Raman Spectroscopic Measurements. Solid-state Raman spectra of compounds **1-4** were collected at the Raman Microscopy Lab (RRID:SCR 019305), University of Colorado-Boulder. Spectra were obtained using a Horiba LabRAM HR Evolution Spectrometer equipped with a 532 nm green laser (frequency-doubled Nd:YAG). Each of the dried compounds was measured as powder samples individually loaded onto glass slides. All spectra were collected between 100 – 650 cm^{-1} by the same spectral resolution utilizing 1800 gr/mm grating. Baseline subtraction and spectral deconvolution was performed in the Horiba LabSpec6 program. Solution-phase Raman spectra of compounds **1-4** were obtained using a Horiba Modular TeraHertz Raman spectrometer.

Frequency Prediction and Analysis. Frequency calculations of vibrational modes were acquired from optimized structures of complexes **1-4**. All calculations were performed using the Gaussian 16 electronic software package with the ωB97X-D density functional and 6-311+g(2d,p) basis set.[6] The structure of each complex was fully optimized from experimental single crystal data and subsequently used for predicating their Raman spectra and vibrational normal modes. Atomic coordinates for those structures are tabulated in Tables S8-S11 Harmonic approximations via this computational method yielded Raman spectra agreeable with the experimental spectra for all computed structures (Figures 5 and S25). All 3N–6 normal modes were predicted for a given structure. Vibrational partition function values, q_{Total}, were calculated for each mode by using the relation (1) where E is the normal mode energy (cm^{-1}), k_B is Boltzmann's constant, and T is temperature (K).

$$q\text{Raman} = \prod \frac{1}{1 - e^{-E/kBT}} \qquad (1)$$

All Other Characterization. ^{1}H NMR spectra were collected on a Bruker Ascend 400 MHz spectrometer. The spectra were referenced using residual protiated solvent signal as an internal standard ($CDCl_3$, 7.26 ppm). UV-Vis and diffuse reflectance spectra were collected by using a Shimadzu UV-2600i UV-Vis spectrophotometer. The absorption spectrum was calculated from reflection spectra by the Kubelka-Munk function.[7] Elemental analyses were performed by Robertson Microlit Analytical Testing Laboratories (Ledgewood, New Jersey, USA). Infrared spectra were recorded on a Nicolet 6700 FTIR spectrometer using a diamond window ATR.

Dynamic light scattering for size measurements was performed using a Malvern Zetasizer Nano ZS instrument equipped with a neon-helium laser (633 nm). The detection angle was 173° and samples were placed in a quartz cell. To obtain a good reproducibility, an optimization was carried out on the number of scans and the acquisition time. Samples were equilibrated at 25 °C for 5 min.

Dynamic Light Scattering (DLS) Measurements and Analyses.

DLS measurements were conducted using 1- mM, 10- mM, and 25 mM solutions of **1**-**4** in $CDCl_3$, CH_2Cl_2, and DMSO, the same solvents used for studying the concentration-dependent properties of ^{59}Co NMR. Despite the solutions of **1**-**4** appearing clear to the eye, they were subjected to filtration and centrifugation to remove any insoluble particles. However, even after these purification steps, DLS measurements still revealed the presence of large particles in the solution. The radius of the particles in solution grew with increasing the concentration. Measuring the concentration of the 1 mM solution posed a challenge due to its low concentration, while the concentrations above 25 mM of solutions presented difficulties because of the high absorbance and dark color of the complexes.[8, 9]

Regarding the relationship between ^{59}Co NMR properties and particle size obtained from DLS measurements, we have noted the following observations:

- Temperature sensitivity does not show any relationship with particle size. The linewidth and the relaxation times, T_1 and T_2 showed variations across the series that did not trend in any discernable way with DLS data.
- The particle sizes for all four compounds in CH_2Cl_2 at various concentrations revealed small aggregate size. For 1 mM solutions, the particle size increased in the order of **4** < **1** < **2** < **3**, and this order changed in 10 mM solutions to **1** < **2** < **4** < **3**. An interesting observation is that two different particle sizes were observed for compound **2**, which might indicate a correlation with the two peaks seen in the ^{59}Co NMR spectra. Although two different sizes were observed for **2** in 10 mM, only one size distribution was observed in 1 mM, which could be attributed to the lower concentration of the solution. Measurements at all concentrations revealed that compound **3** has the largest aggregate size in CH_2Cl_2, which somewhat relates to its low temperature sensitivity in CH_2Cl_2.

- The particle sizes in $CDCl_3$ were found to be slightly larger than those in CH_2Cl_2 for **1**-**4**. For 1 mM solutions, the particle size increased in the order of **4** < **1** < **2** < **3**, similar to the trend in CH_2Cl_2, and this pattern persisted for 10- and 25-mM concentrations. Similar to CH_2Cl_2, two different size distribution was observed for **2**, except for its 1 mM-solutions. Longer T_1 and T_2 values were observed with lower concentrations, corresponding to smaller particle sizes. No direct correlation between concentration and ^{59}Co NMR linewidth was observed.
- The particle sizes of **1**, **2**, and **4** were measured in 1- and 10-mM solutions of DMSO, with the largest size observed in the latter. The particle size increases in the order of **4** < **1** < **2**, with the latter showing particles exceeding 1000 nm in diameter. The ^{59}Co NMR linewidths for all three compounds are widest in DMSO, along with the shortest T_1 and T_2 values (see Table S13, 14). Line broadening in these cases could be attributed to aggregation, as the clustering of molecules alters the chemical environment around the cobalt nuclei.[10] However, this did not hinder our ability to resolve the ^{59}Co NMR peaks in the spectra.

Table S1. Crystallographic information for the structural refinement of **1**.

Empirical formula	$C_{21}H_{27}CoO_6$
Formula weight	434.39 g/mol
Temperature	295(2) K
Crystal system	Monoclinic
Space group	$P2_1/c$
a	8.0692(9) Å
b	15.6356(17) Å
c	15.6240(18) Å
α	90°
β	93.841(4)°
γ	90°
Volume	1966.8(4) $Å^3$
Z	4
ρ_{calc}	1.446 g cm^{-3}
μ	0.907 mm^{-1}
Crystal color	Green
Crystal size	0.081 × 0.084 × 0.128 mm^3
Radiation	MoKα (λ = 0.71073 Å)
2q range for data collection	2.61 to 21.05°
Reflections collected	35186
Independent collections	1902 [R_{int} = 0.0783, R_{sigma} = 0.0276]
Data/restraints/parameters	3290/0/257
Goodness-of-fit on F^2	1.087
Final R indexes [I ≥ 2σ(I)]	R_1 = 0.0664, wR_2 = 0.210
Final R indexes [all data]	R_1 = 0.1381, wR_2 = 0.199
Largest diff. peak/hole	0.9/-0.48 e $Å^{-3}$

Table S2. Temperature sensitivity values for 10 mM solutions of **1** – **4** in various solvents.

Solvent	$\Delta\delta/\Delta T$ (ppm/°C)			
	1	**2**	**3**	**4**
CH_2Cl_2	2.58(1)	2.29(2) / 2.35(2)	0.15(4)	2.37(3)
CD_2Cl_2	2.54(1)	2.19(2) / 2.25(1)	0.2(7)	2.51(2)
$CHCl_3$	2.69(2)	2.68(1) / 2.65(1)	1.41(4)	2.72(3)
$CDCl_3$	2.71(1)	2.69(1) / 2.64(2)	1.55(4)	2.78(2)
MeOH	2.60(2)	2.47(1)	2.0(3)	2.45(2)
DMSO	2.71(3)	2.00(3)	n/a	2.19(2)
Average	2.64(7)	2.39	1.06	2.50

Table S3. The solvent-dependent ^{59}Co NMR parameters of **1** in 10 mM solutions.

Solvent	$\Delta\delta/\Delta T$ (ppm/°C)	$\nu_{1/2}$ (ppm)	$[\Delta\delta/\Delta T]/\nu_{1/2}$ ($°C^{-1}$)
CH_2Cl_2	2.58(1)	1.11	2.32
CD_2Cl_2	2.54(1)	1.18	2.15
$CHCl_3$	2.69(2)	1.75	1.54
$CDCl_3$	2.71(1)	1.12	2.42
MeOH	2.60(2)	1.11	2.34
DMSO	2.71(3)	3.74	0.72
Average	2.33(7)	-	-

Table S4. The solvent-dependent ^{59}Co NMR parameters of **2-I** in 10 mM solutions.

Solvent	$\Delta\delta/\Delta T$ (ppm/°C)	$\nu_{1/2}$ (ppm)	$[\Delta\delta/\Delta T]/\nu_{1/2}$ (°C^{-1})
CH_2Cl_2	2.29(2)	1.89	1.21
CD_2Cl_2	2.19(2)	1.90	1.15
$CHCl_3$	2.68(1)	2.35	1.14
$CDCl_3$	2.69(1)	2.37	1.14
MeOH	2.47(2)	2.53	0.98
DMSO	2.00(3)	8.58	0.23
Average	2.39(3)	-	-

Table S5. The solvent-dependent ^{59}Co NMR parameters of **2-II** in 10 mM solutions.

Solvent	$\Delta\delta/\Delta T$ (ppm/°C)	$\nu_{1/2}$ (ppm)	$[\Delta\delta/\Delta T]/\nu_{1/2}$ (°C^{-1})
CH_2Cl_2	2.35(2)	1.73	1.36
CD_2Cl_2	2.25(2)	1.87	1.20
$CHCl_3$	2.65(1)	2.15	1.23
$CDCl_3$	2.64(2)	2.03	1.30
Average	2.47(2)	-	-

Table S6. The solvent-dependent ^{59}Co NMR parameters of **3** in 10 mM solutions.

Solvent	$\Delta\delta/\Delta T$ (ppm/°C)	$\nu_{1/2}$ (ppm)	$[\Delta\delta/\Delta T]/\nu_{1/2}$ (°C^{-1})
CH_2Cl_2	0.15	1.30	0.12
CD_2Cl_2	0.2	1.12	0.18
$CHCl_3$	1.41	1.34	1.05
$CDCl_3$	1.55	1.32	1.17
MeOH	2.00	1.32	1.52
Average	1.06(8)	-	-

Table S7. The solvent-dependent ^{59}Co NMR parameters of **4** in 10 mM solutions.

Solvent	$\Delta\delta/\Delta T$ (ppm/°C)	$\nu_{1/2}$ (ppm)	$[\Delta\delta/\Delta T]/\nu_{1/2}$ (°C^{-1})
CH_2Cl_2	2.37(3)	1.29	1.84
CD_2Cl_2	2.51(2)	1.30	1.93
$CHCl_3$	2.72(3)	1.74	1.56
$CDCl_3$	2.78(2)	0.85	3.27
MeOH	2.45(2)	1.23	1.99
DMSO	2.19(2)	2.50	0.88
Average	2.50(2)	-	-

Table S8. Computed coordinates of optimized **1** used for Raman frequency calculations. Total Energy = –2650.705984 Hartrees.

Co	0.01485425	0.04271684	-0.01866497
O	-1.60060863	0.02850252	0.96741024
O	-0.38785048	1.55813740	-1.08473578
O	0.70584515	1.21544652	1.29839150
O	1.60996493	-0.13129601	-1.02300993
O	-0.83804720	-1.00869346	-1.34269407
O	0.59912800	-1.39104387	1.06619775
C	-2.50679596	0.87194879	0.74413712
C	-3.78157730	0.86036595	1.55334044
C	-2.53334482	1.91998667	-0.17711630
C	-1.46639614	2.21429854	-1.02579074
C	-1.56740968	3.38765074	-1.96151254
C	1.89127388	1.65381086	1.32215083
C	2.87177532	1.35308670	0.37724715
C	2.65512697	0.48761088	-0.69601088
C	2.22443823	2.56839356	2.46884004
C	-0.91465803	-2.27024467	-1.32117590
C	-1.63723525	-2.89888606	-2.48084551
C	-0.39020545	-3.08353354	-0.31706231
C	0.32398903	-2.58299330	0.77229558
C	-0.43900505	-4.59249924	-0.26756188
C	-4.73819397	1.73333357	0.73296957
C	-3.82673889	2.69178936	-0.06120572
C	-0.04278649	-4.90915685	1.18936742
C	0.81302168	-3.71890775	1.63846798
C	3.92690789	0.32094241	-1.49277320
C	4.79491149	1.50010491	-1.03798740

C	4.30304196	1.83611346	0.38501624
H	-0.62361233	3.52640093	-2.48468093
H	-1.82404648	4.29509257	-1.40994093
H	-2.36328986	3.21345806	-2.69037792
H	2.46623468	3.56576102	2.09211847
H	3.10270374	2.20136979	3.00495803
H	1.37784774	2.63276561	3.14910951
H	-2.53904331	-3.40583336	-2.12747292
H	-1.00649016	-3.65227227	-2.95838406
H	-1.91088021	-2.13447818	-3.20501331
H	-4.13277823	-0.15713291	1.72731621
H	0.27454535	-5.04083083	-0.97041921
H	-1.42201554	-5.00287977	-0.51192978
H	-3.55932456	1.30171391	2.53110927
H	-5.46762994	2.25951124	1.34950625
H	-5.29164462	1.10191386	0.03366616
H	-3.68549994	3.63362057	0.48396432
H	-4.26530983	2.95027670	-1.02830375
H	-0.94427963	-4.95573263	1.80495265
H	0.47322564	-5.86471190	1.28780229
H	1.87561466	-3.87291412	1.41993703
H	0.72909388	-3.47422354	2.69758842
H	4.36956332	-0.64314307	-1.21861311
H	3.72325740	0.29437905	-2.56353095
H	4.61114767	2.35507281	-1.69306491
H	5.86245443	1.28079514	-1.07424885
H	4.39937230	2.90353076	0.59895611
H	4.90142855	1.30742127	1.1377324

Table S9. Computed coordinates of optimized structure of **2** used for Raman frequency calculations. Total Energy = –2993.603603 Hartrees.

Co	-0.02244360	-0.64649003	-0.09545291
O	-0.03162611	-0.87720099	1.77603223
O	1.84709333	-0.74820207	-0.29130705
O	-1.88762492	-0.40826936	-0.00644705
O	-0.07795885	-2.51961520	-0.28850968
O	-0.13936756	-0.51515170	-1.97320534
O	0.15045186	1.20434029	0.21292111
C	1.00426085	-1.07437188	2.47242470
C	2.31508717	-1.12384658	1.99755982
C	-2.73599182	-1.34473830	-0.01677139
C	-2.43482081	-2.70631142	-0.11398629
C	-1.13793084	-3.20523705	-0.24979065
C	-0.17648609	0.57683110	-2.60693297
C	-0.07674523	1.85329350	-2.05065491
C	0.09340986	2.09236318	-0.68454331
C	0.19962288	3.49211815	-0.17753385
C	0.70896352	4.52716719	-0.95734174
C	-0.21346953	3.76138030	1.12555171
C	0.79574559	5.81238194	-0.44490163
C	-0.13916428	5.04840855	1.63153199
C	0.36599505	6.07699797	0.84755089
C	-4.15426416	-0.89552233	0.10530729
C	-5.21680892	-1.64486421	-0.39386428
C	-4.41475798	0.32462918	0.72573663
C	-6.51859125	-1.18564725	-0.26665517
C	-5.71660869	0.77638156	0.86318499
C	-6.77168668	0.02241636	0.36721144

C	4.09143903	-1.01670643	0.23525228
C	5.13186804	-0.66431022	1.09099075
C	4.38652677	-1.43248897	-1.06133081
C	6.44732420	-0.73438369	0.65906528
C	5.70185787	-1.51576732	-1.48660898
C	6.73529664	-1.16616495	-0.62772312
C	0.73700078	-1.26431401	3.94117528
C	-0.92053481	-4.68963448	-0.36750939
C	2.66066383	-0.94856624	0.65382207
C	-0.34963822	0.42569091	-4.09409640
H	3.09824551	-1.33829652	2.70795557
H	-3.24205144	-3.41988783	-0.06001399
H	-0.16265866	2.69821319	-2.71597988
H	1.06590793	4.32683857	-1.96003359
H	-0.59326732	2.94718239	1.72955782
H	1.20497195	6.60848630	-1.05540606
H	-0.47301940	5.25036784	2.64245649
H	0.42987009	7.08301150	1.24544038
H	-5.02897970	-2.57924700	-0.90820679
H	-3.58191789	0.90761516	1.09737818
H	-7.33723131	-1.77084018	-0.66835243
H	-5.90941913	1.72206727	1.35569464
H	-7.79007586	0.37855270	0.46973456
H	4.91593163	-0.30679274	2.09030361
H	3.56988211	-1.69108132	-1.72327594
H	7.24942583	-0.44594399	1.32796944
H	5.92261628	-1.85138204	-2.49298079
H	7.76427873	-1.22533970	-0.96264851
H	0.02228169	-2.07868188	4.07223904
H	1.64463172	-1.48050274	4.50250586

H	0.27545199	-0.35684892	4.33591538
H	-0.24684553	-5.01541766	0.42717012
H	-1.85184714	-5.25074978	-0.30873987
H	-0.42937549	-4.89984880	-1.31960239
H	-1.29094570	-0.09157486	-4.29021501
H	-0.34900454	1.38424861	-4.61055317

Table S10. Computed coordinates of the optimized structure of **3** used for Raman frequency calculations. Total Energy = –3126.113920 Hartrees.

Co	0.00098173	0.00034254	-0.00016756
O	1.31442362	0.74352019	-1.11534839
O	1.20782752	-0.90549250	1.11519133
O	-1.30051017	0.76463581	-1.11525766
O	0.18308536	1.49994216	1.11310471
O	-1.38767418	-0.59041520	1.11500428
O	-0.01165871	-1.50990054	-1.11370932
C	3.05537539	2.86712855	-1.78264916
C	3.37877489	1.38014610	-2.00296260
C	2.55924076	0.58840165	-0.97694122
C	3.16815779	-0.20461631	-0.00031612
C	2.46220803	-0.91252266	0.97641235
C	3.17286271	-1.80370657	2.00213020
C	2.76799195	-1.31875754	3.40253443
C	4.88775227	1.16700817	-1.87969208
C	2.91608583	0.94903782	-3.40309996
C	4.69679919	-1.78551087	1.88016334
C	2.66200218	-3.23678905	1.77959358
C	-4.01373970	1.20651746	-1.77428900

C	-2.52453724	-1.73536698	3.40337971
C	-1.43478406	-4.81508886	-1.87657141
C	0.95470404	-4.08208478	-1.77819800
H	3.37388949	3.19144259	-0.78828000
H	1.98343324	3.04616236	-1.87397487
H	3.57953246	3.47549572	-2.52439174
H	4.24044756	-0.27401858	-0.00041046
H	1.68453686	-1.33596090	3.51953214
H	3.11477995	-0.29656141	3.57638231
H	3.21617568	-1.96422520	4.16244660
H	5.39779051	1.75732967	-2.64485144
H	5.16360350	0.12062169	-2.03087324
H	5.26665218	1.48981600	-0.90714890
H	3.44379026	1.53069404	-4.16347794
H	1.84384534	1.10469946	-3.52111051
H	3.12921846	-0.10940581	-3.57527546
H	5.12640014	-2.43711516	2.64498635
H	5.10429491	-0.78323138	2.03268108
H	5.03192671	-2.15320766	0.90748528
H	1.57589553	-3.27733291	1.87014204
H	3.10353404	-3.90820193	2.52073564
H	2.93716363	-3.59780080	0.78494418
H	-4.45072926	1.32145169	-0.77869547
H	-3.63239056	0.18878699	-1.86531831
H	-4.80515012	1.35458167	-2.51373798
C	-2.88918117	2.23063410	-1.99977683
C	-1.79060943	1.91931802	-0.97620383
C	-1.40775356	2.84425035	-0.00078458
H	-1.88483173	3.80706155	-0.00045339
C	-2.28871076	2.04360740	-3.40143751

H	-3.05873987	2.20807655	-4.15969534
H	-1.88707824	1.03727929	-3.51910022
H	-1.47965512	2.75766529	-3.57725484
C	-3.46011233	3.64366736	-1.87722146
H	-3.92634576	3.81150962	-0.90353273
H	-4.22876430	3.78826956	-2.64034579
H	-2.69295509	4.40618642	-2.03185803
C	1.47396484	3.92620570	1.77299958
H	1.64785656	4.34338386	0.77745573
H	2.05262277	3.00628451	1.86445755
H	1.83516770	4.64566607	2.51255704
C	-0.02218156	3.65177249	1.99771075
C	-0.43949668	2.58892410	0.97427820
C	-0.23794366	3.06082767	3.39931040
H	0.09711603	3.77321561	4.15772477
H	0.31949194	2.13174468	3.51735956
H	-1.29625428	2.84951846	3.57449685
C	-0.80081218	4.96179404	1.87434592
H	-0.65172489	5.43398835	0.90047312
H	-0.45056450	5.66136480	2.63724383
H	-1.87224185	4.81322749	2.02877807
C	-4.13302354	-0.68323218	1.78158478
H	-4.58412929	-0.74073356	0.78731000
H	-3.62459088	0.27741847	1.87167003
H	-4.93463763	-0.72953020	2.52341134
C	-3.14776242	-1.84270835	2.00325278
C	-2.02090893	-1.67339958	0.97720676
C	-1.76084410	-2.63953700	0.00128487
H	-2.35728985	-3.53338677	0.00125695
C	-0.76903649	-2.50983451	-0.97493999

C	-0.49378761	-3.61641697	-2.00007142
C	-0.63364860	-3.00097911	-3.40076019
H	0.03901587	-2.15161681	-3.51896613
H	-1.65606558	-2.65448666	-3.57389949
H	-0.39470716	-3.74988666	-4.16037263
C	-3.89451335	-3.17125244	1.88116279
H	-4.67383254	-3.21713477	2.64578075
H	-3.23066697	-4.02555593	2.03392775
H	-4.38023234	-3.27751904	0.90833427
H	-3.30722057	-1.80101537	4.16368150
H	-1.99745745	-0.78863930	3.52063402
H	-1.81275574	-2.54703172	3.57641750
H	-1.17853918	-5.55342180	-2.64030906
H	-2.47825704	-4.52944440	-2.02967038
H	-1.34675897	-5.30328934	-0.90316038
H	1.64727544	-3.24454601	-1.86947138
H	1.21885202	-4.84116780	-2.51917867
H	1.07460854	-4.51966594	-0.78345746

Table S11. Computed coordinates of the optimized structure of **4** used for Raman frequency calculations. Total Energy = –2418.451742 Hartrees.

Co	0.00004343	0.00005489	-0.00009677
O	1.00490065	1.12878238	-1.13062347
O	1.43592681	-0.47083386	1.13046600
O	-1.12543846	-1.00810600	1.13056595
O	-1.47957096	0.30582801	-1.13056208
O	-0.31053394	1.47884264	1.13027194
O	0.47545855	-1.43446742	-1.13040383
C	-2.29360346	1.26077888	-0.99513940
C	0.57112663	-3.58309485	-2.02675060
C	2.23886199	1.35621005	-0.99470990
C	2.61690485	-0.04671025	0.99516801
C	3.06334333	0.82632453	0.00045784
C	2.81796637	2.28597691	-2.02671378
C	3.58473793	-0.55967998	2.02714652
C	-1.26833400	2.28950631	0.99492750
C	-2.24727504	2.23992357	-0.00014452
C	-3.38787153	1.29713900	-2.02766820
C	-1.30864064	3.38344014	2.02766738
C	0.05478264	-2.61666430	-0.99512052
C	-1.34932694	-2.24273649	0.99467534
C	-0.81723525	-3.06560068	-0.00062834
C	-2.27689293	-2.82461130	2.02707976
H	0.20325938	-4.59534125	-1.86634025
H	0.26710249	-3.23815765	-3.01690510
H	1.66239386	-3.58287533	-2.00025758
H	4.10614705	1.10772757	0.00074085
H	3.87745451	2.47704494	-1.86351562

H	2.26915509	3.22928985	-2.00439525
H	2.67574960	1.84727256	-3.01625399
H	4.59633143	-0.19065660	1.86528868
H	3.24012353	-0.25397208	3.01692491
H	3.58599829	-1.65098113	2.00301922
H	-3.01228819	3.00239049	-0.00013383
H	-4.08471553	2.11756505	-1.86342441
H	-2.93645488	1.39608999	-3.01677821
H	-3.92857687	0.34911944	-2.00735258
H	-2.13157899	4.07738305	1.86356992
H	-0.36257490	3.92749108	2.00758204
H	-1.40603825	2.93139284	3.01663877
H	-1.09548707	-4.10924958	-0.00092236
H	-2.46808844	-3.88374211	1.86157537
H	-3.22028965	-2.27584271	2.00831228
H	-1.83600022	-2.68500581	3.01604126

Table S12. The particle size (hydrodynamic radius) for **1**-**4** obtained from DLS measurements in various concentrations and solvents.

		Particle Size (nm)			
Solvent	Concentration	**1**	**2**	**3**	**4**
CH_2Cl_2	1 mM	37(0.28)	39(1)	47(2)	17(1)
	10 mM	111(17)	128(15) and 2.30(0.3)	213(19)	141(8)
	25 mM	175(22)	231(21)	338(26)	275(20)
$CDCl_3$	1 mM	121(7)	165(5)	177(12)	13(0.02)
	10 mM	295(36)	410(32) and 64(11)	235(17)	27(4)
	25 mM	380(39)	378(73) and 72(17)	414(37)	212(21)
DMSO	1 mM	333(54)	322(102)	*n/s*	10(0.03)
	10 mM	473(196)	983(87)		196(12)
	25 mM	1154(80)	1114(187)		483(64)

Table S13. Concentration-dependent ^{59}Co NMR properties in **1** and **2** obtained in various solvents.

		1			
Solvent	Concentration	$\Delta\delta/\Delta T$ *(ppm/°C)*	$\nu_{1/2}$ *(ppm)*	T_1 *(ms)*	T_2 *(ms)*
CH_2Cl_2	1 mM	2.55(2)	0.75	4.71	3.63
	10 mM	2.57(2)	1.40	4.46	4.06
	100 mM	2.55(3)	1.13	4.27	3.48
$CDCl_3$	1 mM	2.71(3)	1.45	4.21	3.51
	10 mM	2.71(1)	1.45	3.98	2.37
	100 mM	3.50(2)	1.23	3.90	2.81
DMSO	1 mM	2.65(5)	5.09	n/a	
	10 mM	2.63(3)	3.60	1.33	0.97
	100 mM	2.72(4)	4.85	1.58	0.91

		2			
Solvent	Concentration	$\Delta\delta/\Delta T$ *(ppm/°C)*	$\nu_{1/2}$ *(ppm)*	T_1 *(ms)*	T_2 *(ms)*
CH_2Cl_2	1 mM	2.25(1)/2.32(3)	1.70/1.85	2.01(3)/2.15(7)	0.91(2)/0.78(4)
	10 mM	2.29(2)/2.35(2)	1.73/1.89	1.98(2)/2.01(5)	0.98(6)/0.81(4)
	100 mM	2.26(3)/2.25(2)	2.58/2.39	1.77(3)/1.1.77(5)	1.03(4)/1.00(6)
$CDCl_3$	1 mM	2.61(3)	2.35	1.50(4)/0.71(4)	0.51(4)
	10 mM	2.64(2)/2.70(2)	2.37/2.03	1.55(2)/0.80(6)	0.76(5)/n/a
	100 mM	3.39(2)/3.25(3)	2.66/2.42	1.77(3)/1.77(5)	1.03(6)
DMSO	1 mM	2.15(3)	8.78	n/a	
	10 mM	2.00(3)	12.58		
	100 mM	2.04(2)	17.6		

Table S14. Concentration-dependent ^{59}Co NMR properties in **3** and **4** obtained in various solvents.

		3				**4**			
Solvent	Concentration	$\Delta\delta/\Delta T$ *(ppm/°C)*	$\nu_{1/2}$ *(ppm)*	T_1 *(ms)*	T_2 *(ms)*	$\Delta\delta/\Delta T$ *(ppm/°C)*	$\nu_{1/2}$ *(ppm)*	T_1 *(ms)*	T_2 *(ms)*
CH_2Cl_2	1 mM	0.05(2)	1.11	2.95(1)	2.23(2)	2.50(1)	0.65	4.55(4)	3.44(5)
	10 mM	0.12(5)	1.30	2.87(3)	2.16(5)	2.31(6)	1.07	4.89(2)	3.47(2)
	100 mM	0.15(6)	1.04	3.56(4)	2.85(3)	2.53(2)	0.67	4.62(3)	2.81(1)
$CDCl_3$	1 mM	1.54(2)	1.31	2.41(3)	1.97(5)	2.82(2)	0.97	4.29(7)	2.98(2)
	10 mM	1.54(6)	1.32	2.28(3)	1.95(3)	2.78(2)	0.86	4.43(3)	1.41(1)
	100 mM	1.62(3)	1.34	2.21(8)	1.90(2)	2.83(2)	0.91	4.15(5)	3.09(1)
DMSO	not soluble					2.28(2)	2.65	1.07(9)	0.96(2)
						2.63(3)	2.51	0.99(3)	0.95(2)
						2.33(2)	2.75	1.02(5)	0.89(6)

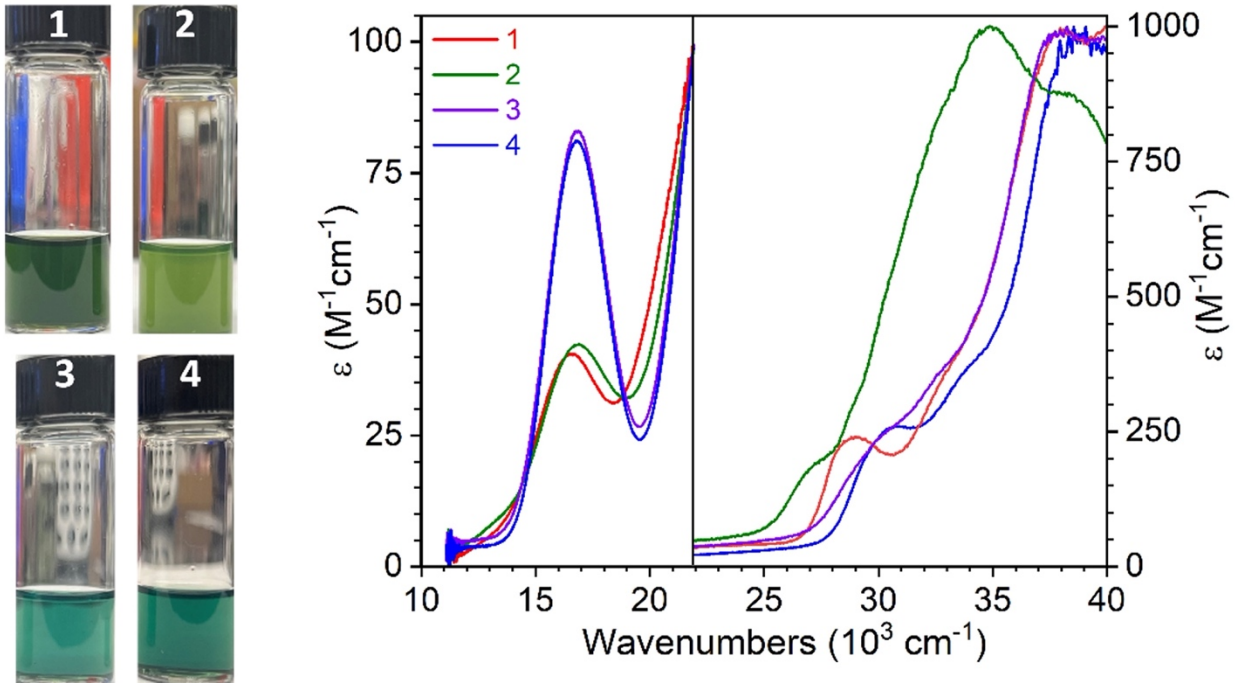

Figure S1. UV-Vis spectra for **1**-**4** in CH_2Cl_2 at room temperature. The solutions in CH_2Cl_2 are also shown to the left of the spectra.

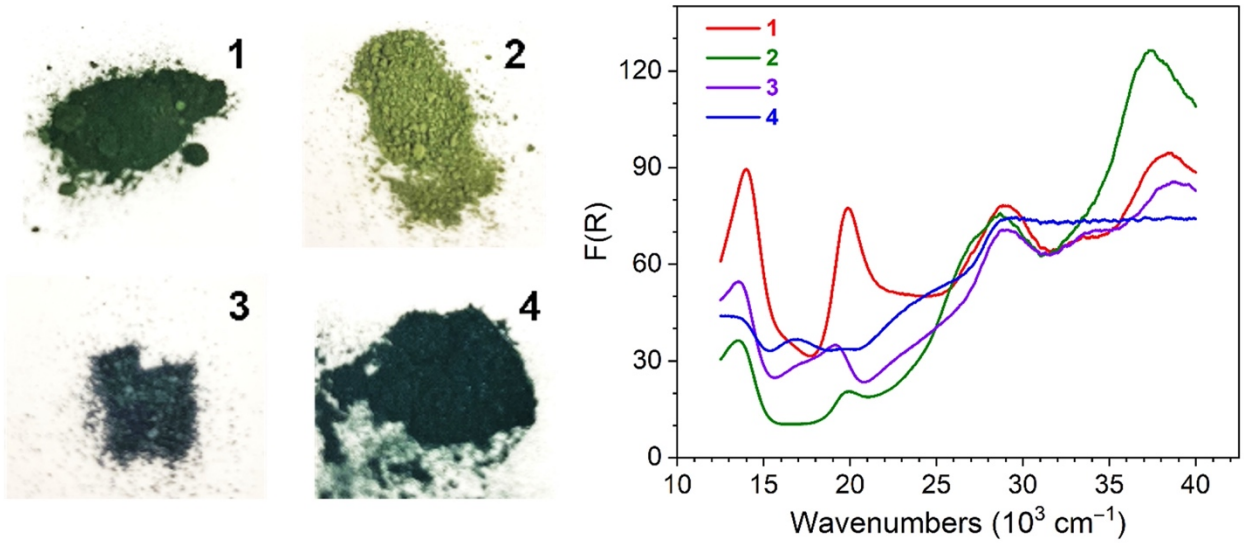

Figure S2. Diffuse reflectance spectra for **1**-**4** at room temperature. The powder sample of each complex are shown to the left of the spectra.

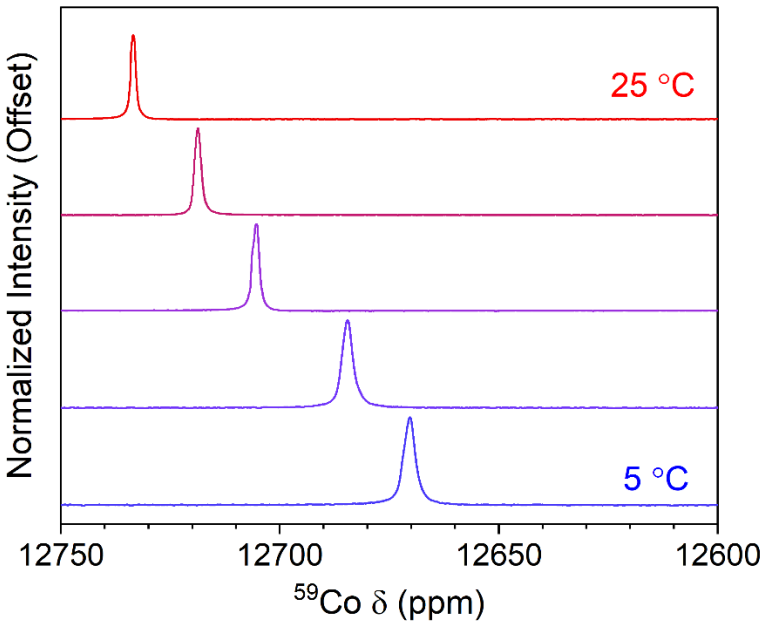

Figure S3. The temperature dependence of the ^{59}Co chemical shift of **1**, collected in $CDCl_3$ (100 mM) in a 500 MHz (^{1}H) NMR spectrometer.

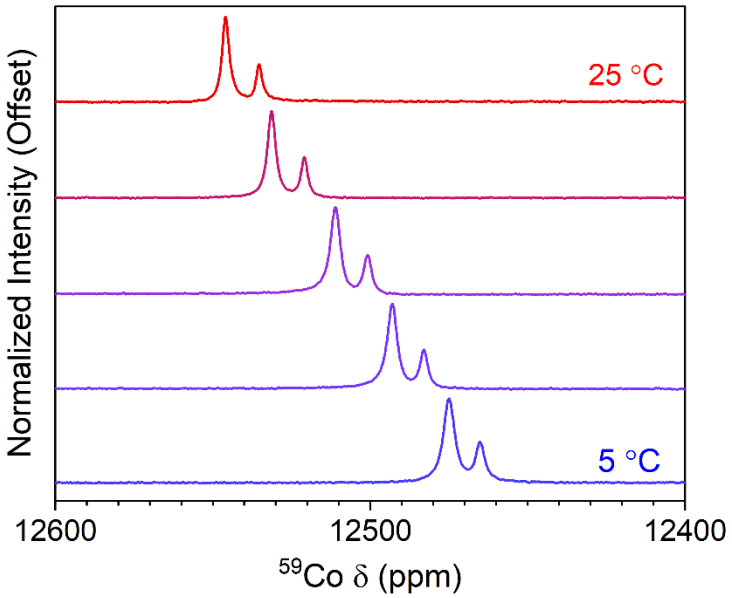

Figure S4. The temperature dependence of the ^{59}Co chemical shift of **2**, collected in $CDCl_3$ (100 mM) in a 500 MHz (^{1}H) NMR spectrometer. The spectra show two peaks corresponding to two different isomers observed for complex **2**. Note that the distance between the two isomers remains the same as the temperature increases.

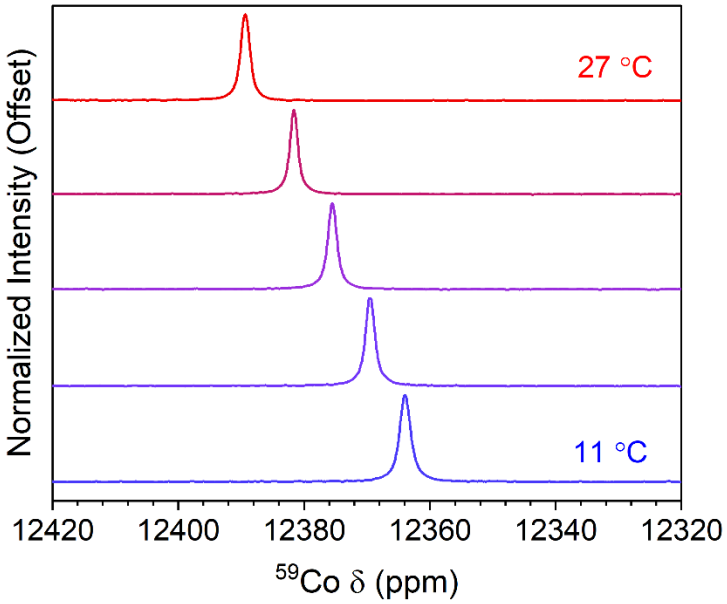

Figure S5. The temperature dependence of the ^{59}Co chemical shift of **3**, collected in $CDCl_3$ (100 mM) in a 500 MHz (^{1}H) NMR spectrometer.

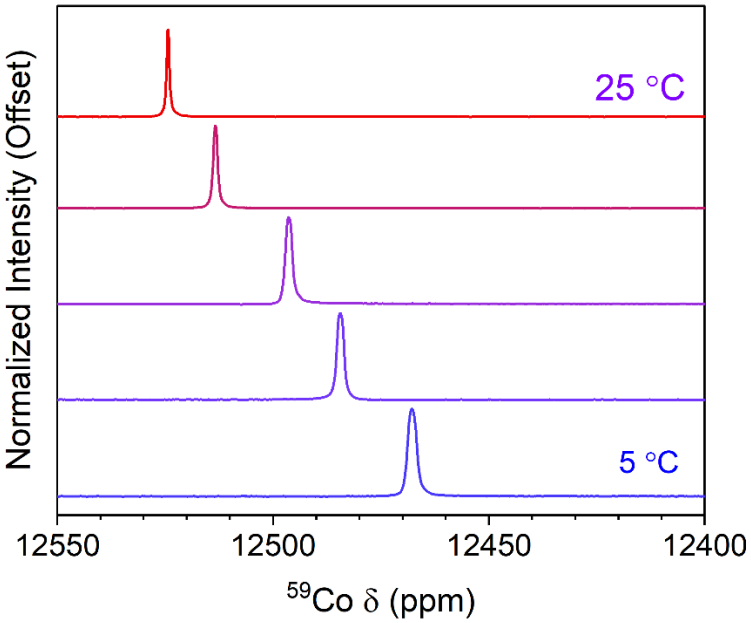

Figure S6. The temperature dependence of the ^{59}Co chemical shift of **4**, collected in $CDCl_3$ (100 mM) in a 500 MHz (^{1}H) NMR spectrometer. Note that the linewidth noticeably sharpens as the temperature increases.

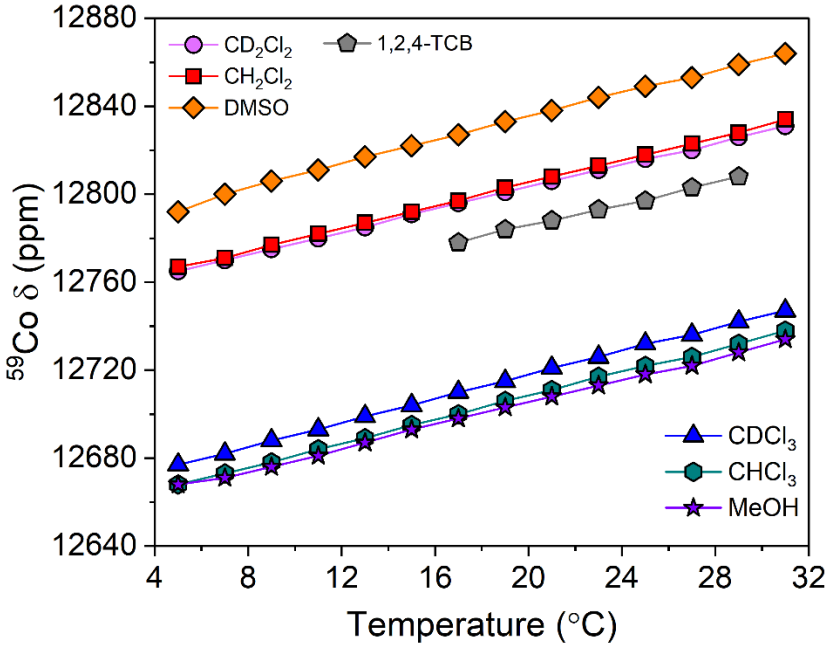

Figure S7. The chemical shift values of **1** (10 mM) as a function of temperature in various solvents. The solid lines are guides for the eye.

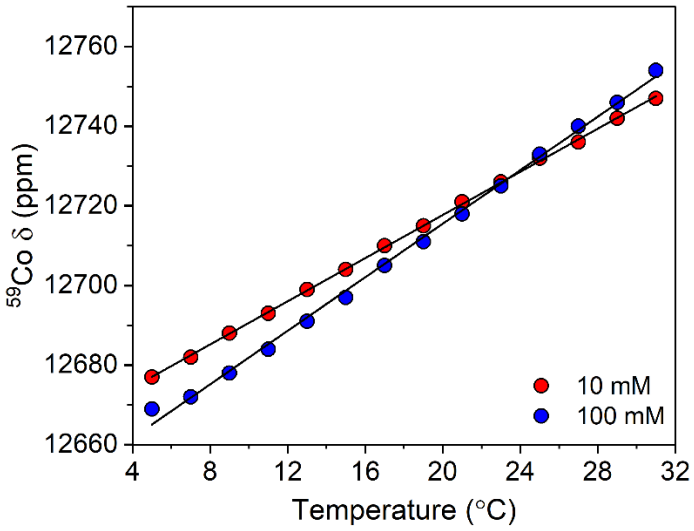

Figure S8. The chemical shift values of **1** in $CDCl_3$ as a function of concentration, recorded using a 500 MHz (^{1}H) NMR spectrometer. The solid black lines are the result of a linear fit.

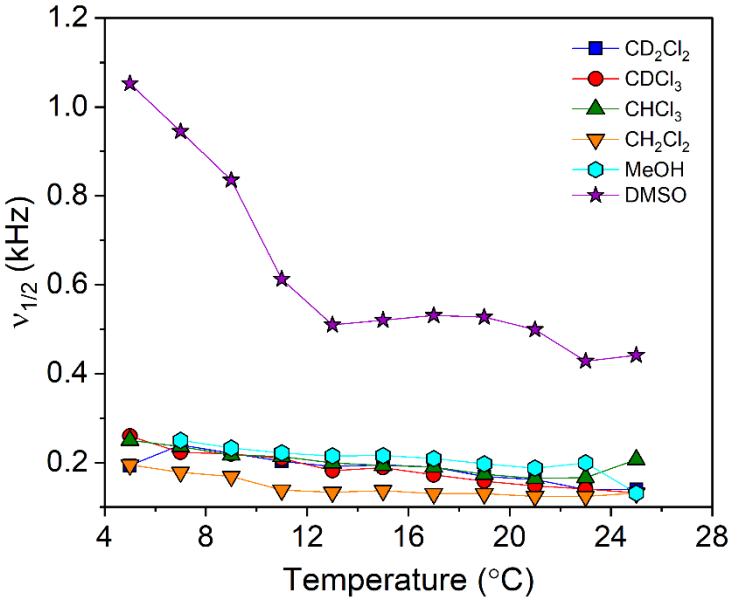

Figure S9. The linewidth values in 10 mM solutions of **1** as a function of temperature in various solvents. The solid lines are guides for the eye.

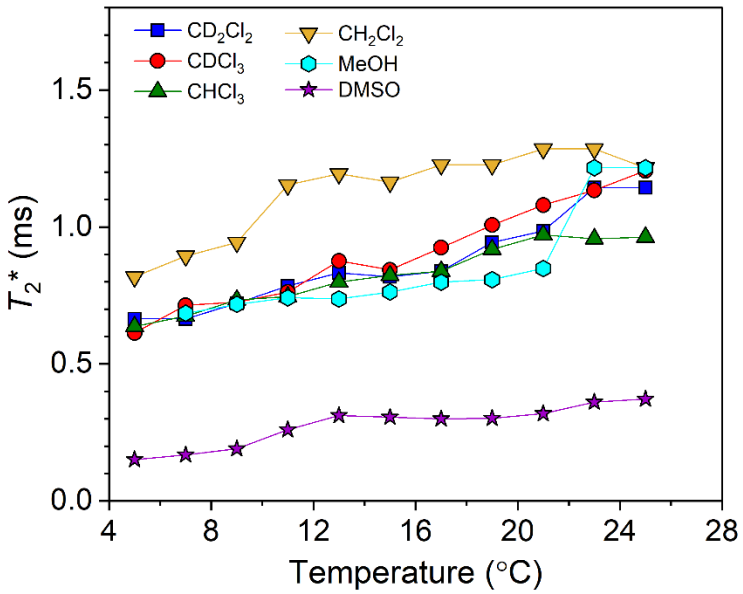

Figure S10. The T_2* values in 10 mM solutions of **1** as a function of temperature in various solvents. The solid lines are guides for the eye.

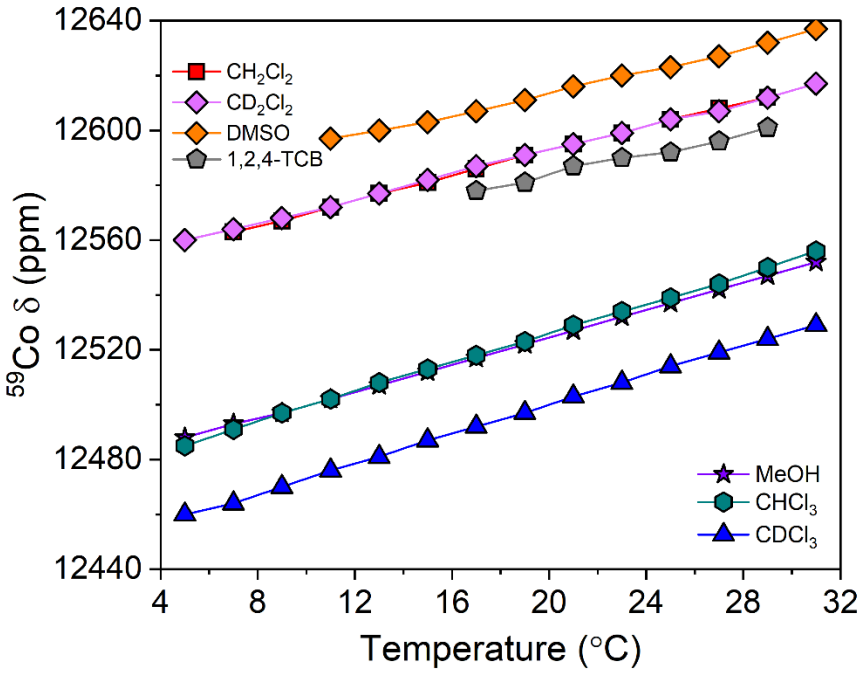

Figure S11. The chemical shift values of **2-I** (10 mM) as a function of temperature in various solvents. The solid lines are guides for the eye.

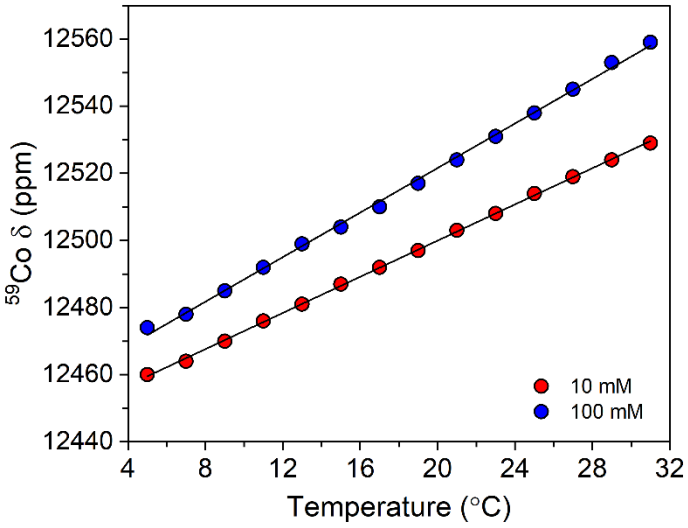

Figure S12. The chemical shift values of **2-I** in $CDCl_3$ as a function of concentration, recorded using a 500 MHz (^{1}H) NMR spectrometer. The solid black lines are the result of a linear fit.

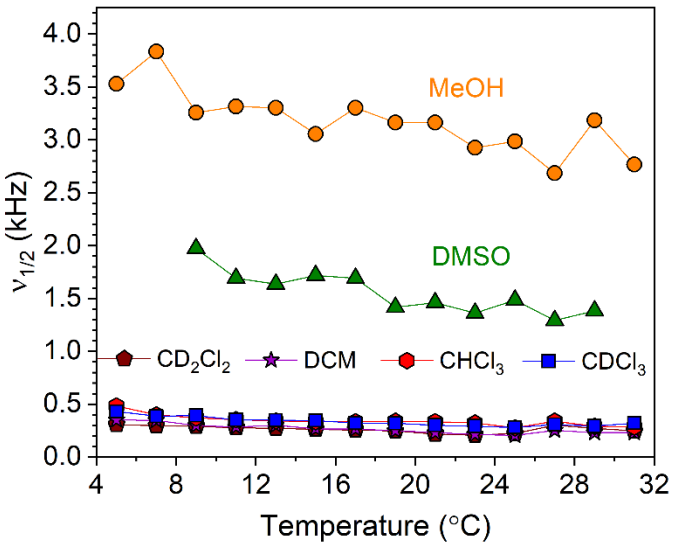

Figure S13. The linewidth values in 10 mM solutions of **2-I** as a function of temperature in various solvents. The solid lines are guides for the eye.

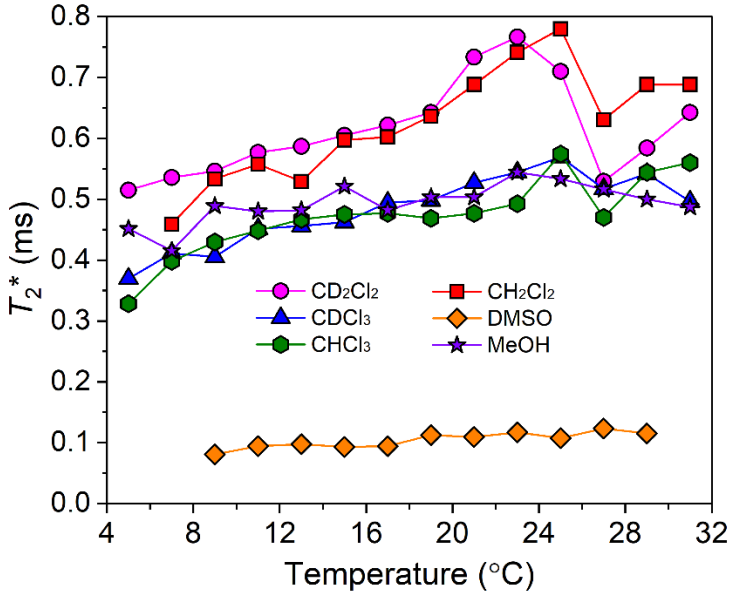

Figure S14. The T_2* values in 10 mM solutions of **2-I** as a function of temperature in various solvents. The solid lines are guides for the eye.

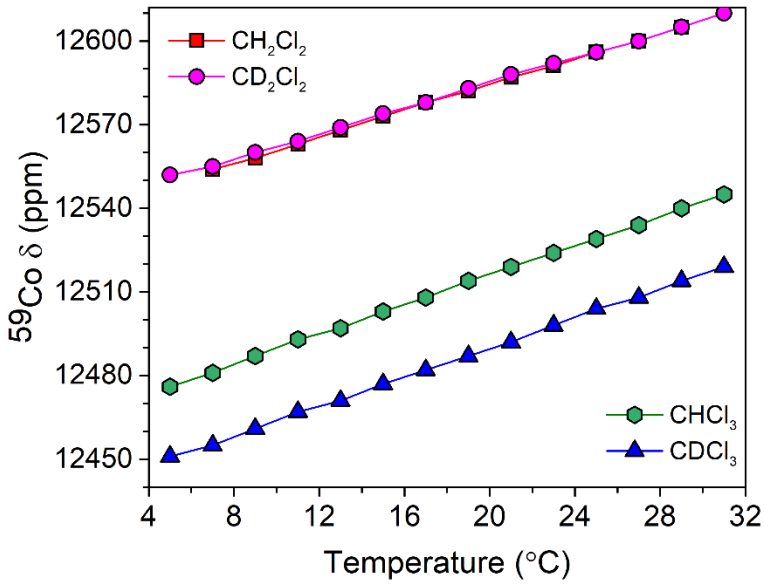

Figure S15. The chemical shift values of **2-II** (10 mM) as a function of temperature in various solvents. The solid lines are guides for the eye.

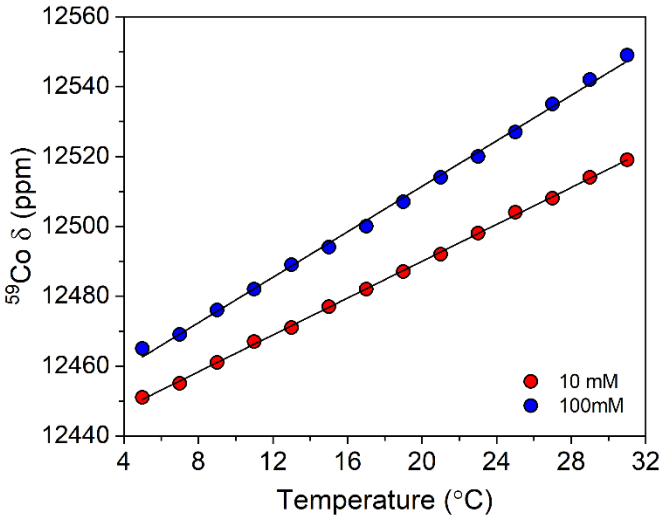

Figure S16. The chemical shift values of **2-II** in $CDCl_3$ as a function of concentration, recorded using a 500 MHz (^{1}H) NMR spectrometer. The solid black lines are the result of a linear fit.

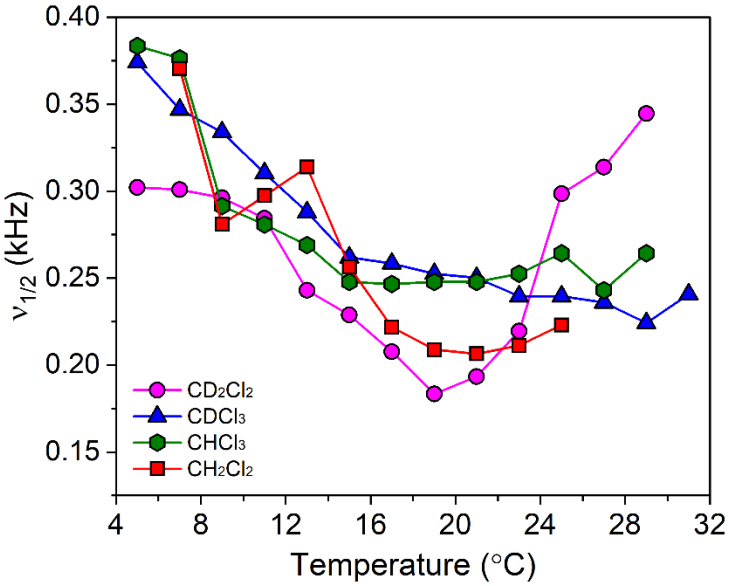

Figure S17. The linewidth values in 10 mM solutions of **2-II** as a function of temperature in various solvents. The solid lines are guides for the eye.

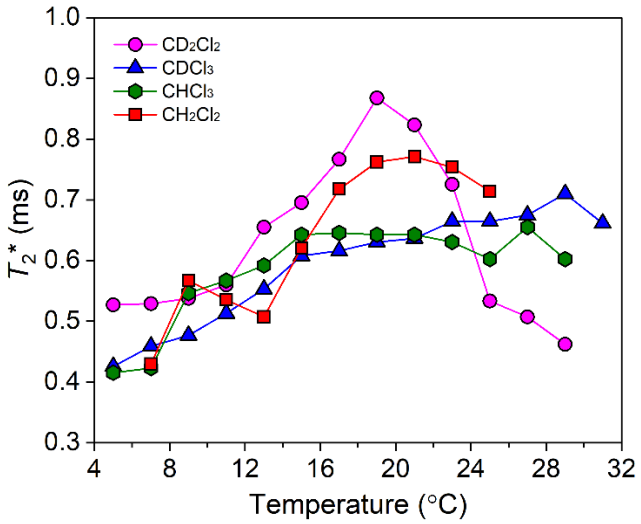

Figure S18. The T_2* values in 10 mM solutions of **2-II** as a function of temperature in various solvents. The solid lines are guides for the eye.

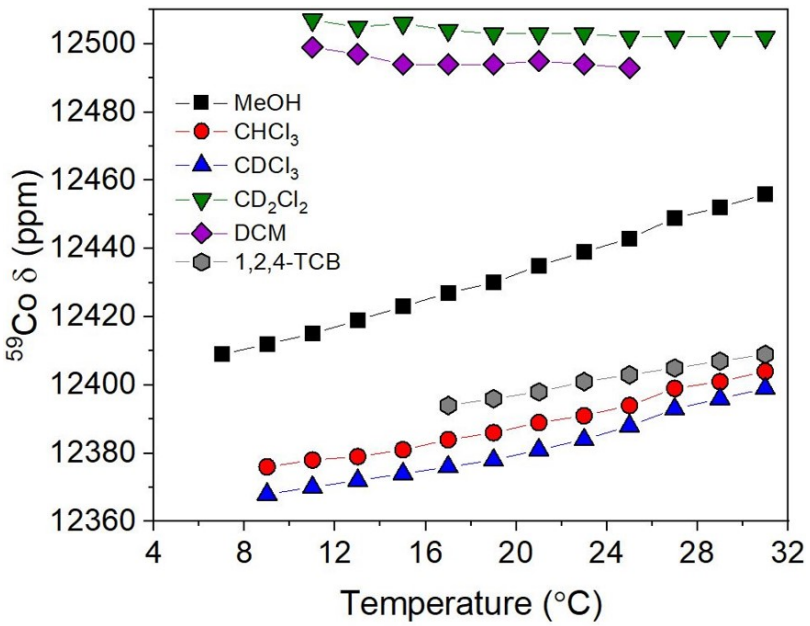

Figure S19. The chemical shift values of **3** as a function of temperature in various solvents. The spectra were collected in 10 mM solutions in a 500 MHz (^{1}H) NMR spectrometer. The solid lines are guides for the eye.

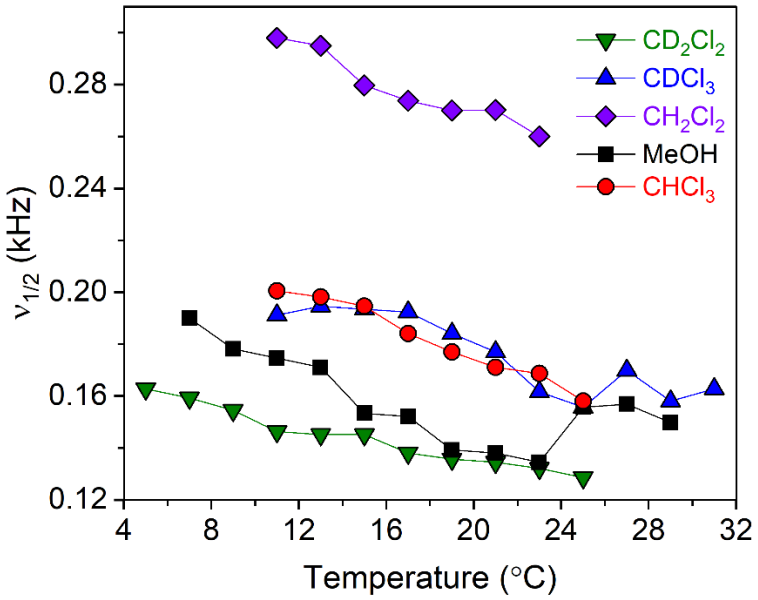

Figure S20. The linewidth values in 10 mM solutions of **3** as a function of various solvents, recorded using a 500 MHz (^{1}H) NMR spectrometer. The solid lines are guides for the eye.

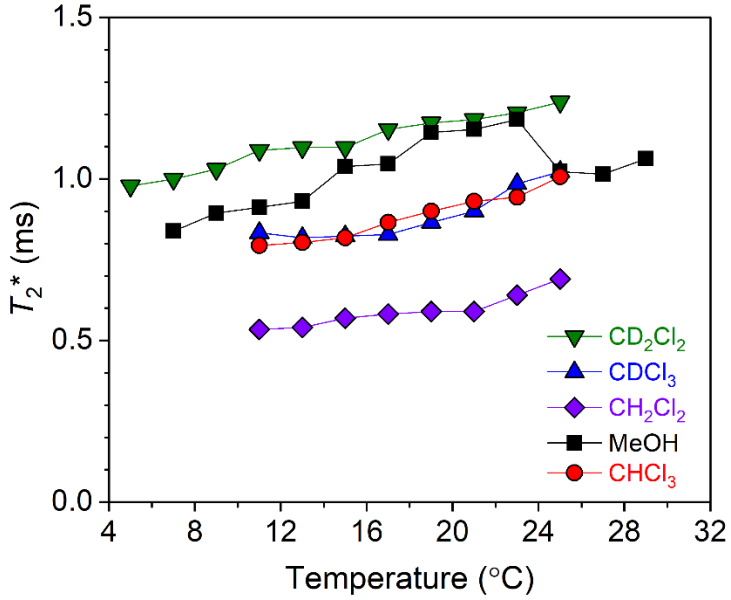

Figure S21. The T_2* values in 10 mM solutions of **3** as a function of various solvents, recorded using a 500 MHz (^{1}H) NMR spectrometer. The solid lines are guides for the eye.

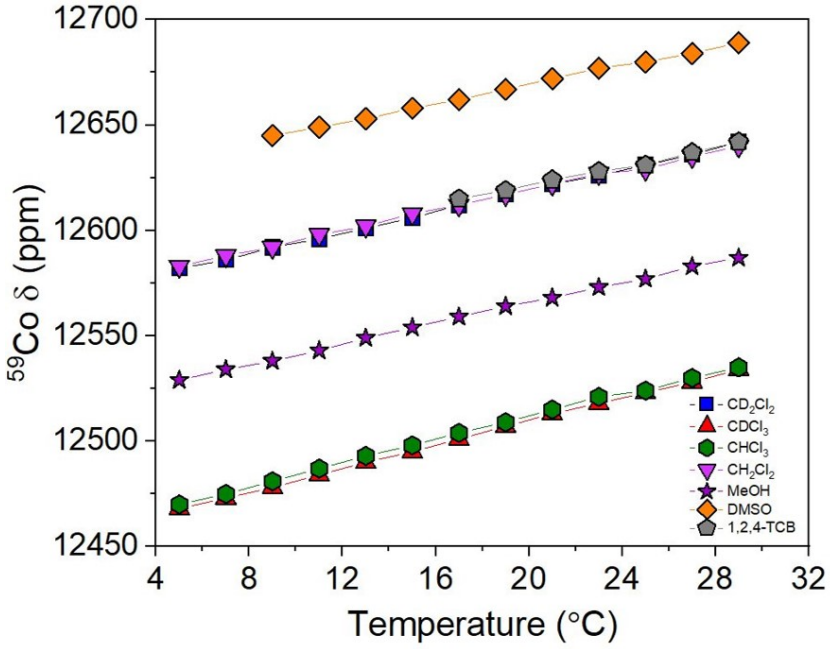

Figure S22. The chemical shift values of **4** as a function of concentration, recorded using a 500 MHz (^{1}H) NMR spectrometer. The solid black lines are the result of a linear fit.

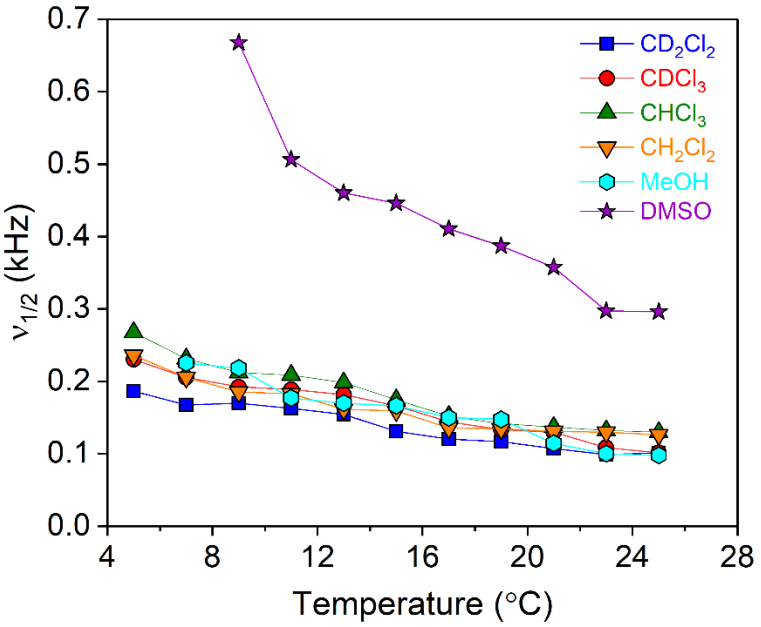

Figure S23. The linewidth values in 10 mM solutions of **4** as a function of various solvents, recorded using a 500 MHz (^{1}H) NMR spectrometer. The solid lines are guides for the eye.

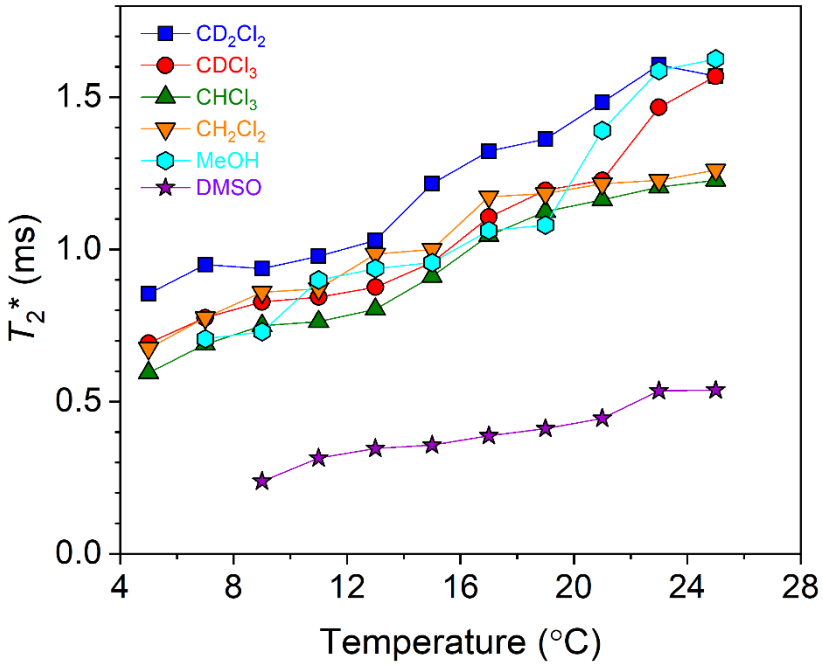

Figure S24. The T_2* values in 10 mM solutions of **4** as a function of various solvents, recorded using a 500 MHz (^{1}H) NMR spectrometer. The solid lines are guides for the eye.

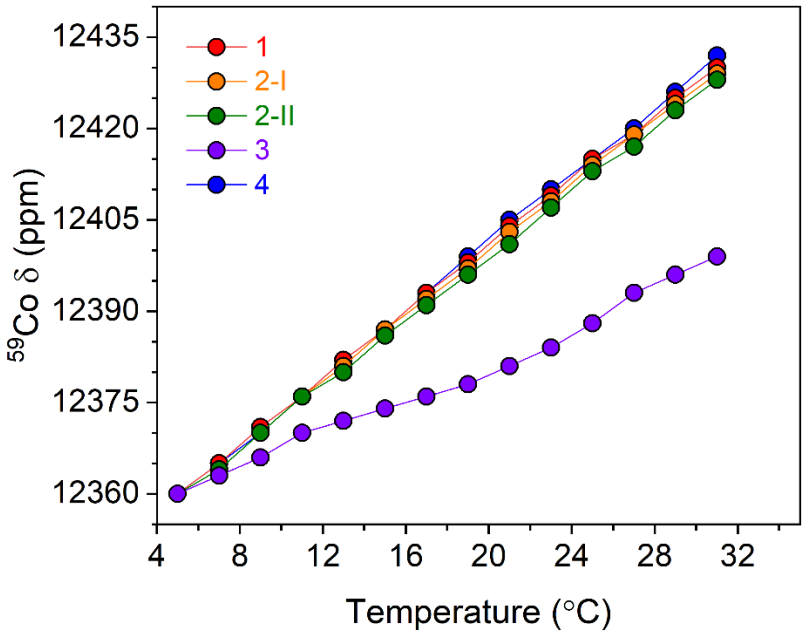

Figure S25. The chemical shift values of **1-4 (**10 mM solutions in $CDCl_3$) as a function temperature, recorded using a 500 MHz (^{1}H) NMR spectrometer.

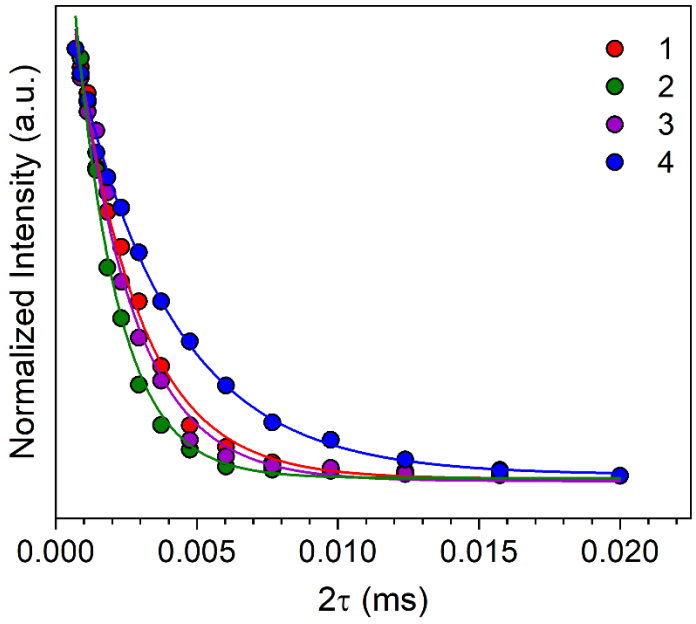

Figure S26. Echo decay data obtained from the CPMG experiment for **1-4**. Decays were fitted with exponential decay functions.

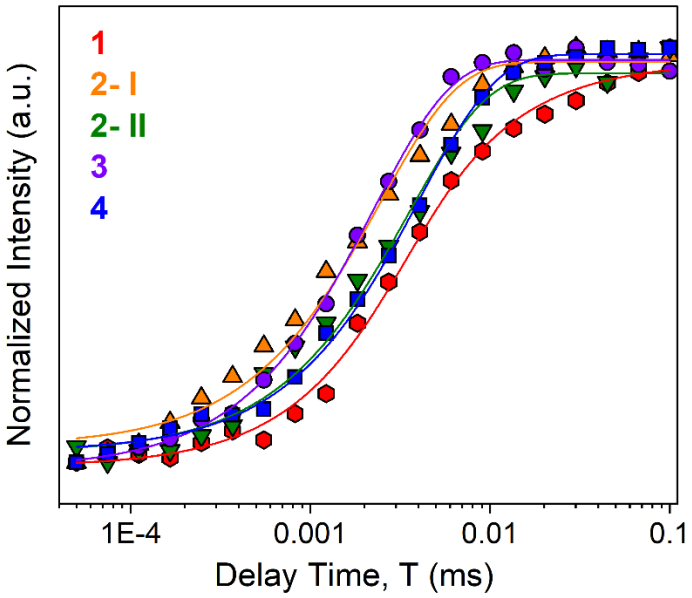

Figure S27. Inversion recovery curves with exponential recovery fits for 100 mM solutions of **1-4** in $CDCl_3$ at 25 °C, plotted on a logarithmic scale.

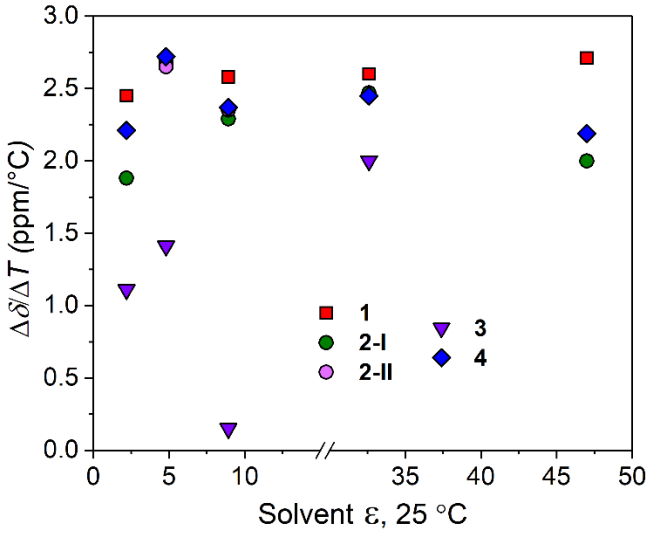

Figure S28: Dependence of the chemical shift sensitivity on solvent polarity for **1-4**.

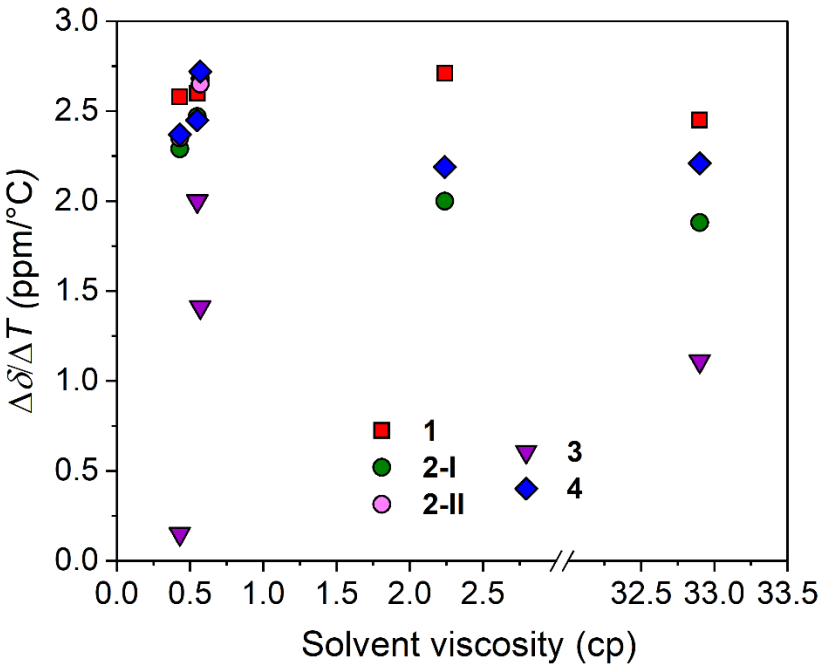

Figure S29: Dependence of the chemical shift sensitivity on solvent viscosity for **1-4**.

References

1. Shalhoub, G. M., Co(acac)3 Synthesis, Reactions, And Spectra: An Experiment For General Chemistry. *J. Chem. Educ.,* 1980, ***57***, 525-526.
2. Sheldrick, G. M., SADABS, Software for Empirical Absorption Correction. 1996.
3. Sheldrick, G. M., Crystal Structure Refinement with SHELXL. *Acta. Crystallogr. C Struct. Chem.,* 2015, ***71***, 3-8.
4. Sheldrick, G. M., SHELXT - Integrated Space-Group and Crystal-Structure Determination. *Acta. Crystallogr. A Found. Adv.,* 2015, ***71***, 3-8.
5. Sheldrick, G. M., A Short History of SHELX. *Acta. Crystallogr.,* 2008, ***64***, 112-122.
6. Krishnan, R.; Binkley, J. S.; Seeger, R.; Pople, J. A., Self-Consistent Molecular Orbital Methods. XX. A Basis Set For Correlated Wave Functions. *Chem. Phys.,* 1980, ***72***, 650-654.
7. Wendlandt, W. W., Hecht, H. G., *Reflectance Spectroscopy*. Interscience Publishiers: New York 1966.
8. Stetefeld, J.; McKenna, S. A.; Patel, T. R., Dynamic Light Scattering: A Practical Guide And Applications In Biomedical Sciences. *Biophys. Rev.,* 2016, ***8***, 409-427.
9. Wishard, A.; Gibb, B. C., Dynamic Light Scattering - An All-Purpose Guide For The Supramolecular Chemist. *Supramol. Chem.,* 2019, ***31***, 608-615.
10. Iida, M.; Sakamoto, A.; Yamashita, T.; Shundoh, K.; Ohkawa, S.; Yamanari, K., NMR Studies on the Aggregation of Mononuclear and Dinuclear Cobalt(III) Amphiphilic Complexes Having Alkyl Chains. *Bull. Chem. Soc. Jpn.,* 2000, ***73***, 2033-2041.